New developments in Sr_2RuO_4

Clifford W. Hicks[#], Michael Nicklas[##], Andrew P. Mackenzie[###]

A series of new experiments have provided more information on the superconductivity of Sr_2RuO_4, which remains one of the great mysteries of condensed matter physics. Superficially contradictory results on whether the order parameter is single- or double-component have caused major new theoretical activity. Separately, using uniaxial stress to tune through a Fermi surface topological transition provides a precisely controllable way to alter electronic correlations, and an opportunity to probe, through transport and thermodynamic measurements, how they emerge and control bulk electronic properties.

Sr_2RuO_4 has emerged as one of the major testing grounds for experiment and theory in condensed matter physics. This is because samples can be grown to a high level of perfection, because it has a superconducting state with T_c = 1.5 K whose origin, after 27 years of inquiry, remains irresistibly mysterious, and because its electronic correlations are in an intermediate regime. Electronic correlations are strong enough to clearly affect the bulk properties of Sr_2RuO_4, and to induce the superconductivity, but also weak enough to be tractable. They renormalize but do not destroy the metallic state. This provides opportunities for precise inquiry.

What also provides opportunities for precise inquiry is the discovery at MPI-CPfS that Sr_2RuO_4 can be driven through a Lifshitz transition, that is, a change in topology of its Fermi surfaces, by uniaxial stress applied along a ⟨100⟩ lattice direction [1, 2]; one of the major research efforts at MPI-CPfS has been to extend the range and precision with which uniaxial stress can be applied to correlated electron materials. This Lifshitz transition has now been directly visualized through angle-resolved photoemission (see Fig. 1), using a platform that employs differential thermal contraction to apply the appropriate uniaxial stress in a compact setup compatible with existing ARPES apparatus [3]. Through use of another newly-developed cell, that incorporates a sensor of the applied force in order to improve the precision of measurement [4], we have shown that this transition occurs at stress σ_{100} = -0.71±0.08 GPa (where the subscript 100 denotes the stress direction) [5].

Since 2018 we have obtained a number of new results on Sr_2RuO_4, with the aims of understanding how the normal metallic state changes as the strength of correlations is tuned with uniaxial stress, and of understanding the superconductivity. Although it will in a way be unfortunate to reach the end of this particular adventure, we are on a path where we will, in time, determine the superconducting order parameter of Sr_2RuO_4, and in the process will gain

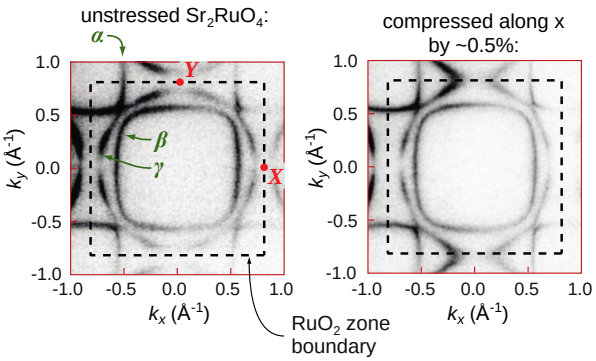

Fig. 1. ARPES visualization of the Fermi surfaces of (left) unstressed Sr_2RuO_4, and (right) Sr_2RuO_4 that has been compressed uniaxially along the x axis by about 0.5%. The γ sheet transitions from an electron-like to an open geometry. The change in Fermi surface topology occurs at a uniaxial stress of $\sigma_{xx} \approx$ -0.71 GPa. (Negative values denote compression.) The conventional labelling of Fermi sheets – α, β, and γ – is shown in the left-hand panel.

much general understanding of unconventional superconductivity, and a range of new experimental capabilities.

One major result, in collaboration with the Technical University of Dresden and in a study that required four years of technical development led by MPI-CPfS, has been the measurement of muon spin relaxation (μSR) on Sr_2RuO_4 placed under uniaxial stress [6]. These measurements have yielded two key findings. Firstly, under uniaxial stress, the onset temperature of time reversal symmetry breaking (TRSB) separates from the superconducting critical temperature T_c [see Fig. 2(a)]. This is consistent with expectations for a chiral order parameter $p_x \pm ip_y$ or $d_{xz} \pm id_{yz}$: under uniaxial stress, the lattice is no longer tetragonal, and so, for example, the d_{xz} and d_{yz} components would no longer onset at the same temperature. It is also an important technical achievement, because the microscopic mechanism by which TRSB superconductivity causes faster muon spin relaxation is not known. (The dominant hypothesis, that TRSB order parameters cause

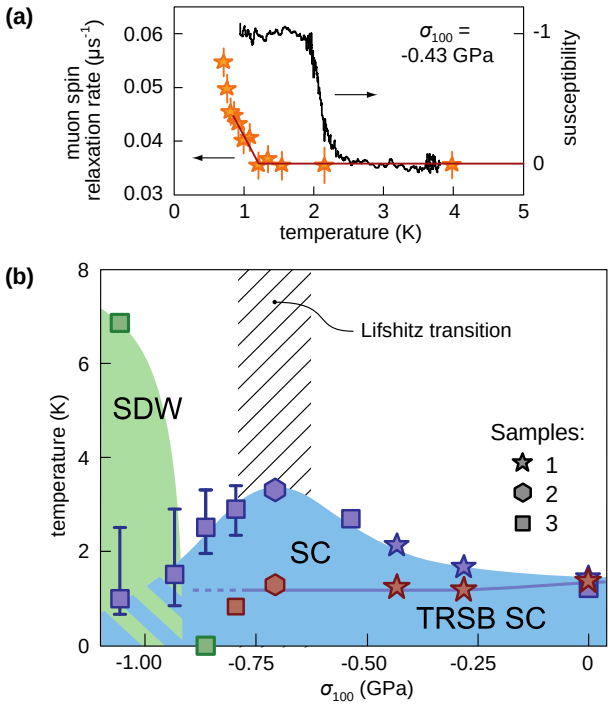

Fig. 2. (a) Muon spin relaxation rate versus temperature for a sample of Sr_2RuO_4 under uniaxial stress σ_{100} = -0.43 GPa. Although T_c is enhanced to 2.0 K, the relaxation rate increases starting at 1.2 K, indicating a split between T_c and the onset of time reversal symmetry breaking. (b) Stress-temperature phase diagram as revealed by muon spin relaxation.

spontaneous fields at defect sites and domain walls, is not consistent with experiments [7].) By showing decisively that the TRSB transition can separate from T_c, we have proved that it is a separate transition, and not an artefact of the superconducting transition itself that is apparent in certain materials by some unknown mechanism.

Our second μSR result is to show that there is static spin density wave order beyond the Lifshitz transition. This confirms that magnetic fluctuations are important in Sr_2RuO_4 and may play a role in the superconductivity. The stress-temperature phase diagram of Sr_2RuO_4, as derived from μSR measurements, is shown in Fig. 2(b).

These μSR results, however, are in apparent contradiction with high-precision heat capacity measurements under uniaxial stress. The heat capacity of uniaxially stressed samples can be measured by an ac method, with a frequency high enough that temperature oscillations are largely confined to the central portion of the sample [8]. Such measurements, performed at MPI-CPfS, place an upper limit on the heat capacity anomaly at any TRSB transition of ~5% that at T_c [9]. Furthermore, scanning SQUID microscopy measurements, in which high precision is obtained by scanning the sample and avoiding regions of inhomogeneity, do not reveal the cusp in the strain dependence of T_c that is expected for a two-component order parameter [10]. This apparent contradiction has led to substantial theoretical activity [11-13].

Collaborative measurements provide further key information. Resonant ultrasound measurements have shown that there is a jump in elastic modulus at T_c that, under the tetragonal lattice symmetry of unstressed Sr_2RuO_4, can only be explained by a two-component order parameter, such as $p_x \pm ip_y$ or $d_{xz} \pm id_{yz}$ [14].

NMR data have shown that there is a drop in Knight shift at T_c that is very difficult to account for with an odd-parity order parameter [15, 16]. This overturns a previous measurement, which was found to be incorrect for a technical reason, and rules out the possibility of $p_x \pm ip_y$ order, which was the dominant hypothesis for most of the history of Sr_2RuO_4. The combination of NMR evidence that the order parameter of Sr_2RuO_4 has even parity and μSR evidence that it has two components suggests a $d_{xz} \pm id_{yz}$ order parameter, but under current understanding this is an unlikely order parameter because it has a horizontal line node at $k_z = 0$, while Sr_2RuO_4 is a layered material with weak interlayer conduction. The superficially contradictory nature of these results has, again, motivated considerable new theoretical effort, including new theories of interorbital pairing that could yield $d_{xz} \pm id_{yz}$ order by a physically plausible mechanism [17, 18].

We now describe new, unpublished results of measurements performed at MPI-CPfS. Firstly, the stress-strain relationship of Sr_2RuO_4 across the Lifshitz transition has been measured; results are shown in Fig. 3(a). Measurement of stress-strain relationships is standard in mechanical engineering, but completely new in correlated electron physics, for a couple of reasons. (1) Measurements should be performed at cryogenic temperatures. (2) The mechanical properties of interesting compounds are often not straightforwardly compatible with high strains. (3) The strains required to induce interesting changes in electronic structure can be very large. We did this measurement using a cell of the design reported in Ref. [4]. It also turns out to be necessary to sculpt the sample, using a focused ion beam, into a dumbell shape, as shown in the inset of Fig. 3(a). Doing so minimizes the sample volume at intermediate strains, which simplifies analysis.

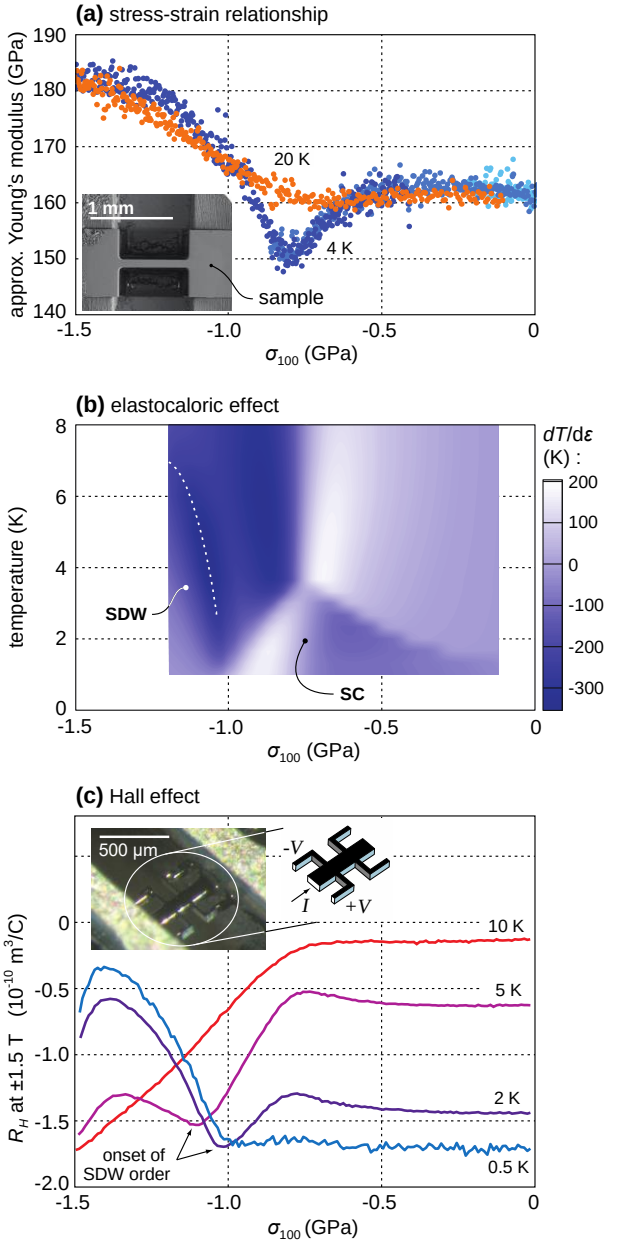

Fig. 3. Evolution of properties of Sr_2RuO_4 across the stress-induced Lifshitz transition. (a) The Young's modulus drops sharply at the Lifshitz transition. The inset shows the sample, which was sculpted with an ion beam. (b) The elastocaloric effect, $dT/d\varepsilon$ under quasi-adiabatic conditions. These data show that for $T > T_c$ entropy is maximum at the Lifshitz transition. (c) The $T \rightarrow 0$ Hall effect, oddly, does not *change across the Lifshitz transition. A picture of the sample is shown in the inset: for precision, the voltage contacts are milled from the sample itself.*

As shown in Fig. 3(a), the Young's modulus (defined as $E = d\sigma/d\varepsilon$, where σ is stress and ε strain) dips sharply at the Lifshitz transition. $E = d^2F/d\varepsilon^2$, where F is free energy, and so the dip in E at the Lifshitz transition shows that the free energy of the electronic system is maximal at the Lifshitz transition.

In Fig. 3(b), we show results of measurement of the elastocaloric effect (ECE). The elastocaloric effect is the change in temperature of a sample under quasi-adiabatic conditions due to applied strain, $dT/d\varepsilon$. It is measured by applying an ac strain and measuring the resulting temperature oscillations [19]. It has the opposite sign to $dS/d\varepsilon$, where S is entropy.

What is seen in Fig. 3(b) is that the electronic entropy, in agreement with intuition, is maximal at the Lifshitz transition for $T > T_c$: $dT/d\varepsilon > 0$ to the right of the transition, and < 0 to the left. Below T_c, entropy at the Lifshitz transition is a minimum, which shows that the average superconducting gap is largest at the Lifshitz transition.

The boundary of the SDW phase is also visible in ECE data. The sign of the ECE along the phase boundary indicates, as expected, that entropy falls as the SDW phase is entered. The boundaries of the SDW and SC phases are seen to approach very closely, but it is as yet unclear whether these phases overlap. The μSR data indicate microscopic coexistence, though due to the large sample size requirement for μSR there is inhomogeneity, and it would be good to confirm this result on a smaller sample.

The ECE and stress-strain relationship both provide thermodynamic information on the effect of tuning to the Lifshitz transition. In Fig. 3(c), we show transport data: the Hall effect versus uniaxial stress. To obtain sufficient precision, as shown in the inset it was necessary to mill the voltage contacts to the sample from the sample itself, using a plasma focused ion beam. By doing so, voltage leads could be placed directly across from each other, almost eliminating contamination from the longitudinal resistivity.

In multi-band metals, the Hall effect is typically not an analyzable quantity, because there are usually too many parameters affecting it to draw firm conclusions. However, by adding a new axis – strain – we do now obtain enough information for meaningful analysis. The data show two surprises: (1) At $T \sim 5$ K and above, the Hall effect becomes more electron-like beyond the Lifshitz transition, despite the fact that an electron-like Fermi surface changes to an open Fermi surface at the transition. (2) In the $T \rightarrow 0$ limit, there is no change in the Hall effect across the Lifshitz transition despite the change in Fermi surface topology; a strong change is

only observed at larger stress, where the magnetic order onsets.

The change in Hall coefficient at higher T is potentially explainable by a model of Sr_2RuO_4 as a Hund's metal, in which the scattering time depends on orbital content rather than position in k space [20]. Correlations are thought to be strongest on sections of Fermi surface with xy orbital weight – mostly the γ sheet [see Fig. 1(a)] – because it is the xy band that has a high Fermi-level density of states near the Van Hove points X and Y, where Fermi velocity is suppressed. Stronger scattering within the γ sheet suppresses its contribution to the Hall effect, making the Hall effect less electron-like than the Fermi surface topology would suggest. Beyond the Lifshitz transition, a sharp fall in scattering, due to a suppression of correlations, on the convex portions of the γ sheet would make the Hall coefficient more strongly electron-like. A weakening of correlations would also explain the large drop in resistivity observed beyond the Lifshitz transition [21]. These data show how strain-tuning allows much more precise inquiry into the effect of correlations than was possible previously.

Finally, we show in Fig. 4 some results from compression along the c axis. For this measurement, samples must be long and thin along the c axis, which is technically challenging because the cleave plane of Sr_2RuO_4 is the ab plane. We used a plasma focused ion beam to sculpt a sample into a dumbell shape as shown in the inset of Fig. 4(a). By concentrating stress into a narrow neck, a uniaxial stress of -3.2 GPa was attained – a compression along the c axis of ≈1.5%.

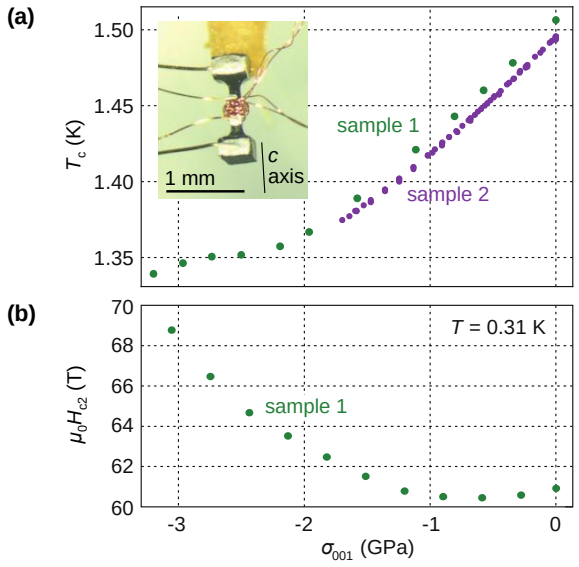

Fig. 4. (a) T_c, and (b) H_{c2} versus c-axis uniaxial stress. The increase in H_{c2} shows that the density of states increases with c-axis compression, and yet T_c decreases. The inset in panel (a) is a photograph of sample 2 before mounting in the strain cell: it has been sculpted into a dumbell shape, to concentrate stress in the neck region. Electrical contacts and coils for susceptibility measurements are also visible.

Electronic structure calculations show that c-axis compression reduces the energy of the xy relative to the xz and yz bands, enlarging the γ sheet and pushing it towards the zone boundary at both the X and Y points. The associated increase in the density of states might be expected to raise T_c, but instead, T_c falls. H_{c2} increases, showing that, as predicted, c-axis compression increases the Fermi level density of states. The contrasting responses to a- and c-axis stress, both of which increase the Fermi-level density of states, provides an important new constraint on the superconducting order parameter.

External Cooperation Partners

Prof. S. E. Brown, University of California at Los Angeles; Prof. M. Garst, Karlsruhe Institute of Technology; Prof. H.-H. Klauss, Technical University of Dresden; Prof. Y. Maeno, Kyoto University; Prof. K. A. Moler, Stanford University; Prof. B. J. Ramshaw, Cornell University; Prof. J. Schmalian, Karlsruhe Institute of Technology.

References

[1] *Strong increase in T_c of Sr_2RuO_4 under both tensile and compressive strain, C. W. Hicks, D. O. Brodsky, E. A. Yelland, A. S. Gibbs, J. A. N. Bruin, M. E. Barber, S. D. Edkins, K. Nishimura, S. Yonezawa, Y. Maeno, and A. P. Mackenzie, Science **344** (2014) 283, doi.org/10.1126/science.1248292*

[2] *Strong peak in T_c of Sr_2RuO_4 under uniaxial pressure, A. Steppke, L. Zhao, M. E. Barber, T. Scaffidi, F. Jerzembeck, H. Rosner, A. S. Gibbs, Y. Maeno, S. H. Simon, A. P. Mackenzie, and C. W. Hicks, Science **355** (2017) eaaf9398, doi.org/10.1126/science.aaf9398*

[3]* *Direct observation of a uniaxial stress-driven Lifshitz transition in Sr_2RuO_4, V. Sunko, E. A. Morales, I. Marković, M. E. Barber, D. Milosavljević, F. Mazzola, D. A. Sokolov, N. Kikugawa, C. Cacho, P. Dudin, et al., npj Quant. Materials **4** (2019) 46, doi.org/10.1038/s41535-019-0185-9*

[4]* *Piezoelectric-based uniaxial pressure cell with integrated force and displacement sensors, M. E. Barber, A. Steppke, A. P. Mackenzie, and C. W. Hicks, Rev. Sci. Inst. **90** (2019) 023904, doi.org/10.1063/1.5075485*

[5]* *Role of correlations in determining the Van Hove strain in Sr_2RuO_4, M. E. Barber, F. Lechermann, S. V. Streltsov, S. L. Skornyakov, S. Ghosh, B. J. Ramshaw, N. Kikugawa,*

D. A. Sokolov, A. P. Mackenzie, C. W. Hicks, and I. I. Mazin, Phys. Rev. B ***100*** *(2019) 245139, doi.org/10.1103/PhysRevB.100.245139*

[6]* *Split superconducting and time-reversal symmetry-breaking transitions in Sr_2RuO_4 under stress, V. Grinenko, S. Ghosh, R. Sarkar, J.-C. Orain, A. Nikitin, M. Elender, D. Das, Z. Guguchia, F. Brückner, M. E. Barber, et al., Nat. Phys.* ***17*** *(2021) 748, doi.org/10.1038/s41567-021-01182-7*

[7] *Limits on superconductivity-related magnetization in Sr_2RuO_4 and $PrOs_4Sb_{12}$ from scanning SQUID microscopy, C. W. Hicks, J. R. Kirtley, T. M. Lippman, N. C. Koshnick, M. E. Huber, Y. Maeno, W. M. Yuhasz, M. B. Maple, and K. A. Moler, Phys. Rev. B* ***81*** *(2010) 214501, doi.org/10.1103/PhysRevB.81.214501*

[8]* *Heat-capacity measurements under uniaxial pressure using a piezo-driven device, Y.-S. Li, R. Borth, C. W. Hicks, A. P. Mackenzie, and M. Nicklas, Rev. Sci. Inst.* ***91*** *(2020) 103903, doi.org/10.1063/5.0021919*

[9]* *High-sensitivity heat-capacity measurements on Sr_2RuO_4 under uniaxial pressure, Y.-S. Li, N. Kikugawa, D. A. Sokolov, F. Jerzembeck, A. S. Gibbs, Y. Maeno, C. W. Hicks, J. Schmalian, M. Nicklas, and A. P. Mackenzie, Proc. Nat. Acad. Sciences USA* ***118*** *(2021) e2020492118, doi.org/10.1073/pnas.2020492118*

[10]* *Micron-scale measurements of low anisotropic strain response of local T_c in Sr_2RuO_4, C. A. Watson, A. S. Gibbs, A. P. Mackenzie, C. W. Hicks, and K. A. Moler, Phys. Rev. B* ***98*** *(2018) 094521.*

[11] *Knight shift and leading superconducting instability from spin fluctuations in Sr_2RuO_4, A. T. Rømer, D. D. Scherer, I. M. Eremin, P. J. Hirschfeld, and B. M. Andersen, Phys. Rev. Lett.* ***123*** *(2019) 247001.*

[12] *A proposal for reconciling diverse experiments on the superconducting state in Sr_2RuO_4, S. A. Kivelson, A. C. Yuan, B. Ramshaw, and R. Thomale, npj Quantum Materials* ***5*** *(2020) 43, doi.org/10.1038/s41535-020-0245-1*

[13] *Inhomogeneous time-reversal symmetry breaking in Sr_2RuO_4, R. Willa, M. Hecker, R. M. Fernandes, and J. Schmalian, arXiv (2020) 2011.01941.*

[14]* *Thermodynamic evidence for a two-component superconducting order parameter in Sr_2RuO_4, S. Ghosh, A. Shekhter, F. Jerzembeck, N. Kikugawa, D. A. Sokolov, M. Brando, A. P. Mackenzie, C. W. Hicks, and B. J. Ramshaw, Nat. Phys.* ***17*** *(2021) 199, doi.org/10.1038/s41567-020-1032-4*

[15]* *Normal state ^{17}O NMR studies of Sr_2RuO_4 under uniaxial stress, Y. Luo, A. Pustogow, P. Guzman, A. P. Dioguardi, S. M. Thomas, F. Ronning, N. Kikugawa, D. A. Sokolov, F. Jerzembeck, A. P. Mackenzie, et al., Phys. Rev. X* ***9*** *(2019) 021044, doi.org/10.1103/PhysRevX.9.021044*

[16]* *Constraints on the superconducting order parameter in Sr_2RuO_4 from oxygen-17 nuclear magnetic resonance, A. Pustogow, Y. Luo, A. Chronister, Y.-S. Su, D. A. Sokolov, F. Jerzembeck, A. P. Mackenzie, C. W. Hicks, N. Kikugawa, S. Raghu, et al., Nature* ***574*** *(2019) 72, doi.org/10.1038/s41586-019-1596-2*

[17] *Stabilizing even-parity chiral superconductivity in Sr_2RuO_4, H. G. Suh, H. Menke, P. M. R. Brydon, C. Timm, A. Ramires, and D. F. Agterberg, Phys. Rev. Research* ***2*** *(2020) 032023(R), doi.org/10.1103/PhysRevResearch.2.032023*

[18] *Shadowed triplet pairings in Hund's metals with spin-orbit coupling, J. Clepkens, A. W. Lindquist, and H.-Y. Kee, Phys. Rev. Research* ***3*** *(2021) 013001, doi.org/10.1103/PhysRevResearch.3.013001*

[19] *AC elastocaloric effect as a probe for thermodynamic signatures of continuous phase transitions, M. S. Ikeda, J. A. W. Straquadine, A. T. Hristov, T. Worasaran, J. C. Palmstrom, M. Sorensen, P. Walmsley, and I. R. Fisher, Rev. Sci. Inst.* ***90*** *(2019) 083902, doi.org/10.1063/1.5099924*

[20] *Hall coefficient signals orbital differentiation in the Hund's metal Sr_2RuO_4, M. Zingl, J. Mravlje, M. Aichhorn, O. Parcollet, and A. Georges, npj Quantum Materials* ***4*** *(2019) 35, doi.org/10.1038/s41535-019-0175-y*

[21] *Resistivity in the vicinity of a Van Hove singularity: Sr_2RuO_4 under uniaxial pressure, M. E. Barber, A. S. Gibbs, Y. Maeno, A. P. Mackenzie, and C. W. Hicks, Phys. Rev. Lett.* ***120*** *(2018) 076602, doi.org/10.1103/PhysRevLett.120.076602*

[#] C.Hicks.1@bham.ac.uk
[##] nicklas@cpfs.mpg.de
[###] mackenzie@cpfs.mpg.de